viruses

MDPI

Article

SARS-CoV-2 Omicron Induces Enhanced Mucosal Interferon Response Compared to other Variants of Concern, Associated with Restricted Replication in Human Lung Tissues

Or Alfi [1,2,3], Marah Hamdan [1], Ori Wald [4], Arkadi Yakirevitch [5,6], Ori Wandel [1], Esther Oiknine-Djian [1], Ben Gvili [5], Hadas Knoller [5], Noa Rozendorn [5], Hadar Golan Berman [7], Sheera Adar [7], Olesya Vorontsov [1,2,3], Michal Mandelboim [8,9], Zichria Zakay-Rones [2], Menachem Oberbaum [10], Amos Panet [2] and Dana G. Wolf [1,3,*]

1 Clinical Virology Unit, Hadassah Hebrew University Medical Center, Jerusalem 91120, Israel; or.alfi@mail.huji.ac.il (O.A.); marah.hamdan@mail.huji.ac.il (M.H.); oriwandel@gmail.com (O.W.); djianesther@gmail.com (E.O.-D.); lesyav@gmail.com (O.V.)
2 Department of Biochemistry, Institute for Medical Research Israel Canada, Faculty of Medicine, The Hebrew University, Jerusalem 9112102, Israel; zichriar@ekmd.huji.ac.il (Z.Z.-R.); amospa@ekmd.huji.ac.il (A.P.)
3 Lautenberg Center for General and Tumor Immunology, Faculty of Medicine, The Hebrew University, Jerusalem 9112102, Israel
4 Department of Cardiothoracic Surgery, Hadassah Hebrew University Medical Center, Jerusalem 91120, Israel; oriwald@hadassah.org.il
5 Department of Otorhinolaryngology, Sheba Medical Center, Ramat Gan 52621, Israel; arkadiyak@gmail.com (A.Y.); bengvili@gmail.com (B.G.); hknoller@gmail.com (H.K.); noa.rzn@gmail.com (N.R.)
6 Sackler Faculty of Medicine, Tel Aviv University, Tel Aviv 6997801, Israel
7 Department of Microbiology and Molecular Genetics, Institute for Medical Research Israel-Canada, Faculty of Medicine, The Hebrew University, Jerusalem 9112102, Israel; hadar.golan@mail.huji.ac.il (H.G.B.); sheera.adar@mail.huji.ac.il (S.A.)
8 Central Virology Laboratory, Ministry of Health, Sheba Medical Center, Ramat Gan 52621, Israel; michal.mandelboim@sheba.health.gov.il
9 School of Public Health, Sackler Faculty of Medicine, Tel Aviv University, Tel Aviv 6997801, Israel
10 The Center for Integrative Complementary Medicine, Shaare Zedek Medical Center, Jerusalem 9103102, Israel; menachem@oberbaums.com
* Correspondence: danaw@ekmd.huji.ac.il

check for updates

Citation: Alfi, O.; Hamdan, M.; Wald, O.; Yakirevitch, A.; Wandel, O.; Oiknine-Djian, E.; Gvili, B.; Knoller, H.; Rozendorn, N.; Golan Berman, H.; et al. SARS-CoV-2 Omicron Induces Enhanced Mucosal Interferon Response Compared to other Variants of Concern, Associated with Restricted Replication in Human Lung Tissues. *Viruses* **2022**, *14*, 1583. https://doi.org/10.3390/v14071583

Academic Editors: Elmostafa Bahraoui and Remi Planes

Received: 28 June 2022
Accepted: 20 July 2022
Published: 21 July 2022

Publisher's Note: MDPI stays neutral with regard to jurisdictional claims in published maps and institutional affiliations.

Abstract: SARS-CoV-2 Omicron variant has been characterized by decreased clinical severity, raising the question of whether early variant-specific interactions within the mucosal surfaces of the respiratory tract could mediate its attenuated pathogenicity. Here, we employed ex vivo infection of native human nasal and lung tissues to investigate the local-mucosal susceptibility and innate immune response to Omicron compared to Delta and earlier SARS-CoV-2 variants of concern (VOC). We show that the replication of Omicron in lung tissues is highly restricted compared to other VOC, whereas it remains relatively unchanged in nasal tissues. Mechanistically, Omicron induced a much stronger antiviral interferon response in infected tissues compared to Delta and earlier VOC-a difference, which was most striking in the lung tissues, where the innate immune response to all other SARS-CoV-2 VOC was blunted. Notably, blocking the innate immune signaling restored Omicron replication in the lung tissues. Our data provide new insights to the reduced lung involvement and clinical severity of Omicron.

Keywords: Omicron; organ culture; interferon response; nasal organ culture; lung organ culture; COVID-19; SARS-CoV-2

1. Introduction

The recently evolved SARS-CoV-2 Omicron variant has been shown to exhibit increased transmissibility and escape from humoral immunity generated by previous infections and vaccines [1–4]. Importantly, accumulating clinical–epidemiological observations

demonstrated that Omicron is associated with a milder disease compared with Delta and earlier variants of concern (VOC) [2,5,6]. The decreased clinical severity of Omicron has been partly attributed to the presence of pre-existing population immunity [2]. Additionally, it was proposed that intrinsic viral factors could play a part in its milder disease course. This notion was suggested by studies in animal models showing that Omicron infection caused milder lung pathology [7–9] and by the reported inefficient replication of Omicron in human alveolar organoids and ex vivo infected lung tissues [10,11]. It was further shown that Omicron enters cells by a different route than other variants and does not spread as efficiently by fusion, thereby limiting viral infection in the lungs, where cell fusion plays a role in viral transmission [2,10–13]. These studies highlight the multifactorial yet incompletely resolved mechanisms underlying the decreased pathogenicity of Omicron.

The innate immune response is known to play a key role in SARS-CoV-2 infection outcomes [14–16]. We, therefore, reasoned that the early innate immune responses to Omicron within the respiratory tract could potentially mediate its milder clinical severity. To investigate the local-mucosal susceptibility and response to Omicron, we used our recently established ex vivo SARS-CoV-2 infection models in native 3D human nasal and lung tissues, which recapitulate viral infection in the upper and lower respiratory tract [17]. We identified distinctive patterns of susceptibility and antiviral interferon responses to Omicron, compared to Delta and precedent VOC, which were most remarkable in lung tissues, and provide new clues to the reduced clinical severity of Omicron.

2. Materials and Methods

2.1. Cells and Viruses

Simian kidney Vero E6 (ATCC CRL-1586), Calu-3 (ATCC HTB-55), Madin-Darby Canine Kidney (MDCK, ATCC CCL-34™) cells, and H1299-ACE2 overexpressed cells (kindly provided by Dr. Alex Sigal) [1] were maintained in Dulbecco's Modified Eagle Medium (DMEM; Biological Industries, Beit Haemek, Israel), supplemented with 10% fetal bovine serum, 2 mM L-Glutamine, 10 IU/mL Penicillin, and 10 µg/mL streptomycin (Biological Industries, Beit Haemek, Israel). An early pandemic SARS-CoV-2 D614G isolate (GISAID ID: EPI_ISL_10125580), an Alpha B.1.1.7 isolate (GISAID ID: EPI_ISL_10125211), a Delta, B.1.617.2 isolate (GISAID ID: EPI_ISL_9837720) and an Omicron B.1.1.529 isolate (GISAID ID: EPI_ISL_7869197) were isolated from positive nasopharyngeal swab samples. The Beta variant B.1.351 (GISAID ID: EPI_ISL_678615) was generously provided by Dr. Alex Sigal. All viruses were isolated and propagated (2 passages) in Calu-3 cells and sequence verified. Influenza virus A(H1N1) pdm09 (NIBRG-121xp, Cat# 09/268; obtained from NIBSC, Potters Bar, UK) was propagated in MDCK cells. The virus titers of cleared infected cells and infected tissue supernatants were determined by a standard plaque assay on H1299-ACE2 cells (SARS-CoV-2) [1] or MDCK cells (influenza virus).

2.2. Preparation and Infection of Nasal Turbinate and Lung Organ Cultures

Nasal turbinate and lung organ cultures were prepared and infected as previously described [16]. In brief, inferior nasal turbinate tissues were obtained from consented patients undergoing turbinectomy procedures, and lung tissues (the tumor-free margins) were obtained from consented patients undergoing lobectomy operations. The study was approved by the Hadassah Medical Center (#0296-20-HMO) and the Sheba Medical Center (#2832-15-SMC) Institutional Review Boards. Fresh tissues were kept on ice until further processed on the same day. The tissues were sectioned by a microtome (McIlwain Tissue Chopper; Ted Pella, Inc., Redding, CA, USA) into thin slices (250 µm-thick slices; each encompassing ~10 cell layers), and incubated in 0.3 mL of enriched RPMI medium (Biological Industries, Beit Haemek, Israel) (for the nasal turbinate tissues) or DMEM/F-12 medium (Biological Industries, Beit Haemek, Israel) with MEM Vitamin Solution (Biological Industries, Beit Haemek, Israel) (for the lung tissues), with 10% fetal bovine serum, 2.5 µg glucose/mL, 2 mM glutamine, 10 IU/mL penicillin, 10 µg/mL streptomycin, and 0.25 µg/mL amphotericin B, at 37 °C, 5% CO_2. The tissues were processed and infected on the same day (the

day of harvesting; Day 0). For infection of the organ cultures, the tissues were placed in 48-well plates and inoculated with the respective virus (1×10^5 PFU/well in 0.3 mL) for 12 h to allow effective viral adsorption. For UV-inactivated virus exposure experiments in the lung tissues, the medium containing 1×10^5 PFU in 0.3 mL was pre-exposed to UV for 1 h and validated for complete loss of infectivity. Following viral adsorption, the cultures were washed three times (in 0.3 mL of complete medium) and further incubated for the duration of the experiment, with replacement of the culture medium every 2 to 3 days. Tissue viability was monitored by the mitochondrial dehydrogenase enzyme (MTT) assay as previously described [17]. All infection and tissue processing experiments were performed in a BSL-3 facility.

2.3. Ruxolitinib Treatment

The lung tissues were pretreated for 16 h with 5 μM ruxolitinib (TargetMol Chemicals Inc., Boston, MA, USA) before infection and further incubation in the presence of 5 μM ruxolitinib for the indicated duration of the experiments.

2.4. Whole-Mount Tissue Immunofluorescence

Tissues were fixed in 4% formaldehyde for 24 h, washed in PBS, and transferred to 80% ethanol. The tissues were permeabilized by 0.3% Triton-X100 in PBS (PBST) and further incubated with Animal-Free Blocker® (Vector laboratories, Cat# SP-5035-100) to block nonspecific antibody binding, followed by incubation with the primary antibodies in Animal-Free Blocker® at room temperature overnight. The tissues were then washed 4 times in PBST, incubated with the secondary antibodies in Animal-Free Blocker® at room temperature overnight, washed 4 times with PBST, and incubated with 4′,6-diamidino-2-phenylindole (DAPI, 10 uM, Abcam, Cambridge, UK, Cat# ab228549) as a nuclear stain. The following primary antibodies were used: α-E-Cadherin (Mouse monoclonal, 1:100, Abcam, ab1416; for the detection of epithelial cells), α-SARS-CoV-2 Nucleocapsid (Rabbit monoclonal, 1:500, Abcam, ab271180). The following secondary antibodies were used: Donkey anti-Mouse IgG pre-adsorbed, Alexa Fluor® 568 (1:250, Abcam, Cat# ab175700), Goat anti-Rabbit IgG Highly Cross-Adsorbed Alexa Fluor Plus 647 (1:250, Thermo Fisher Scientific, Waltham, CA, USA, Cat# A32733). For tissue clearing, stained preparations were dehydrated with 100% Ethanol for 1h and later submerged and mounted in ethyl cinnamate (99%; Sigma, Tokyo, Japan, Cat# 112372), as previously described [17]. Whole-mount tissues were visualized using a Nikon A1R confocal microscope and were analyzed using NIS Elements software (Nikon, Tokyo, Japan).

2.5. RNA Purification and Quantification

Infected- and mock-infected organ cultures and the respective supernatants were flash-frozen and stored at −80 °C until assayed. RNA was extracted using NucleoSpin RNA Mini kit for RNA purification (Macherey-Nagel, Düren, Germany, Cat #740955.250) according to the manufacturer's instructions and subjected to reverse transcription using High-Capacity cDNA Reverse Transcription Kit (Thermo Fisher Scientific, Cat#). Quantitative real-time (RT)-PCR was performed on a Quantstudio 3™ (Thermo Fisher Scientific) instrument, using Fast SYBR™ Green Master Mix (Thermo Fisher Scientific, Cat# 4385614) or TaqMan™ Fast Advanced Master Mix (Thermo Fisher Scientific, Cat# 4444558). The employed primers and probe sequences are listed in Table S1.

2.6. Statistical Analysis

All data, presented as means ± standard errors of the mean (SEM), were analyzed using a paired, two-tailed *t*-test in GraphPad Prism 9 software (GraphPad Software Inc., San Diego, CA, USA). *p* values of <0.05 were considered significant.

3. Results

3.1. SARS-CoV-2 Omicron Exhibits Restricted Replication in Human Lung Tissues

Nasal and lung tissues maintained viable as integral organ cultures as described [17], were infected in parallel with Omicron and Delta, using the same viral inoculum. Viral replication kinetics were monitored between 2 and 72 h post-infection by quantitative measurements of tissue-associated viral sub-genomic (sg)-mRNA and secreted infectious virus progeny, as described [17]. To control for the expected tissue-to-tissue variations (reflecting the natural diversity of different donors), we used five and four independent lung and nasal tissues, respectively. Whereas Omicron and Delta demonstrated similar replication kinetics in the nasal tissues (Figure 1A), the replication of Omicron in the lung tissues was highly restricted compared to the productive replication of Delta (Figure 1B). This relative replication restriction, which was most apparent at late times post-infection, was confirmed by confocal microscopy analysis, showing the near-absence of infected cells in Omicron-infected lung tissues (Figure 1C). The Delta replication kinetics in the lung tissues was overall similar to those of D614G, Alpha, and Beta variants (Figure S1). Hence, the restricted replication of Omicron in the lung tissues distinguished it from all precedent SARS-CoV-2 VOC examined.

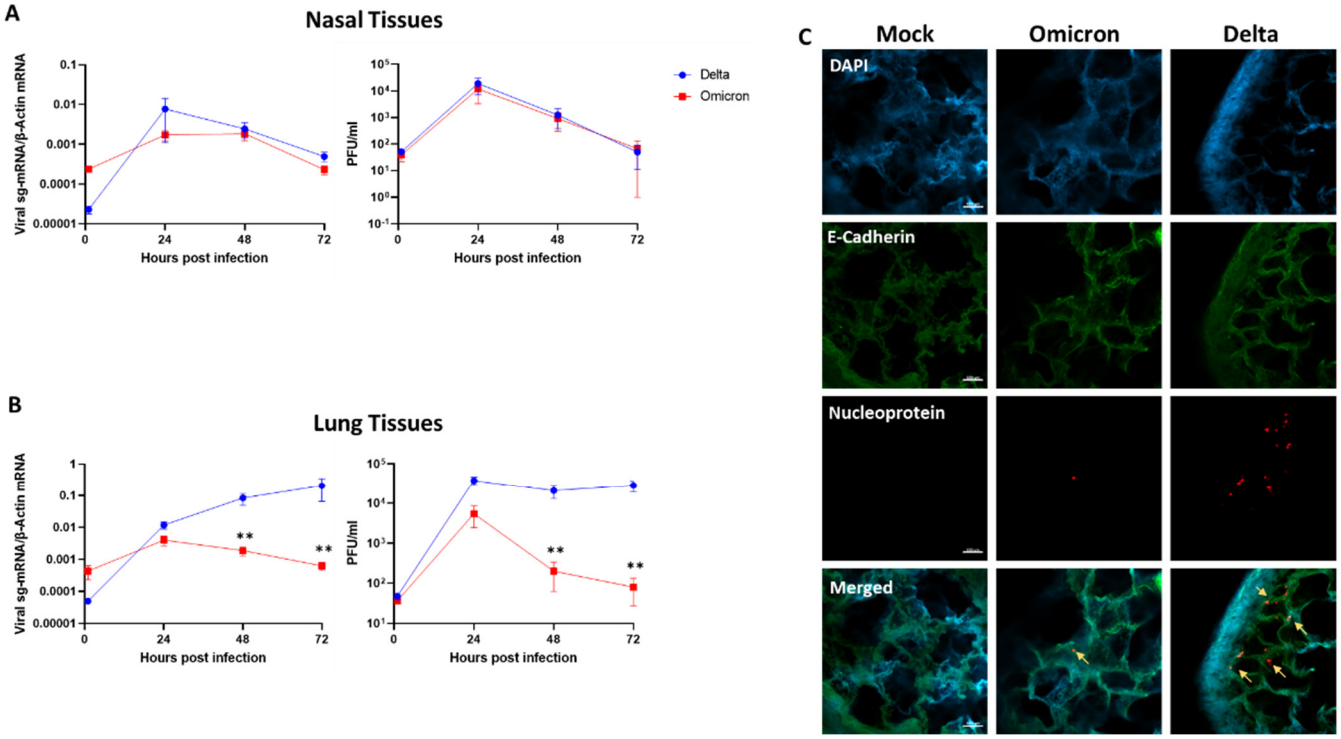

Figure 1. SARS-CoV-2 Omicron and Delta replication kinetics in human nasal and lung tissues. Nasal (**A**) and lung (**B**) organ cultures were (each) infected in parallel with Omicron and Delta (10^5 PFU/well). The levels of tissue-associated viral sub-genomic (sg)-mRNA (left panels) and infectious virus progeny released from the same infected tissues (right panels) represent mean values (±SEM) of four and five independent nasal and lung tissues, respectively, each tested in four biological replicates. (**C**) Representative confocal micrographs of whole-mount lung tissues at 72 h post-infection. Whole-mount tissues were visualized using a Nikon A1R confocal microscope and were analyzed using NIS Elements software (Nikon). Scale bar = 100 μm. **, $p < 0.01$. Statistics were performed using multiple paired, two-tailed Student's *t*-test.

3.2. Omicron Elicits Enhanced Antiviral Interferon Response in Human Respiratory Tissues

We previously showed that SARS-CoV-2 infection (the ancestral isolate USA-WA1/2020) induced a robust innate immune response in nasal tissues, albeit a highly restricted innate immune response in lung tissues [17]. In order to compare the innate immune response

triggered by Omicron versus Delta, we examined the expression of interferons (IFNs) and representative antiviral interferon-stimulated genes (ISG) in lung tissues upon parallel infection with the two variants. The selected ISG included MX1, IFI6, ISG15, and IFIT1, which were previously demonstrated to exhibit broad-acting antiviral activities and inhibit SARS-CoV-2 replication [18,19]. Interestingly, employing RT-qPCR, we showed that Omicron infection elicited a vigorous lung-tissue innate immune response, with substantial induction of the expression of IFNλ and ISGs (Figure 2A). We could not detect upregulation of IFNα and IFNβ in the infected tissues (data not shown). The strong interferon response induced by Omicron was in sharp contrast to the low ISG response of the same lung tissues to Delta. We also showed, in parallel infection experiments, that the restricted lung-tissue response to Delta was common to all other VOC tested, including D614G, Alpha, and Beta (whereas the same lung tissues still exhibited a strong response to influenza virus) (Figure S2). In line with the enhanced interferon response triggered by Omicron in the lung tissues, Omicron also induced some enhancement of the interferon response in infected nasal tissues, compared with Delta (Figure S3). However, it was notable that the nasal tissues (unlike the lung tissues) already exhibited a strong response to Delta (Figure S3), which was generally consistent with our previous observations [17]. Thus, the enhancement of the innate immune response to Omicron, compared to other VOC, was most remarkable in the lung tissues, where the response to all other SARS-CoV-2 VOC was largely restricted and less remarkable in the nasal tissues.

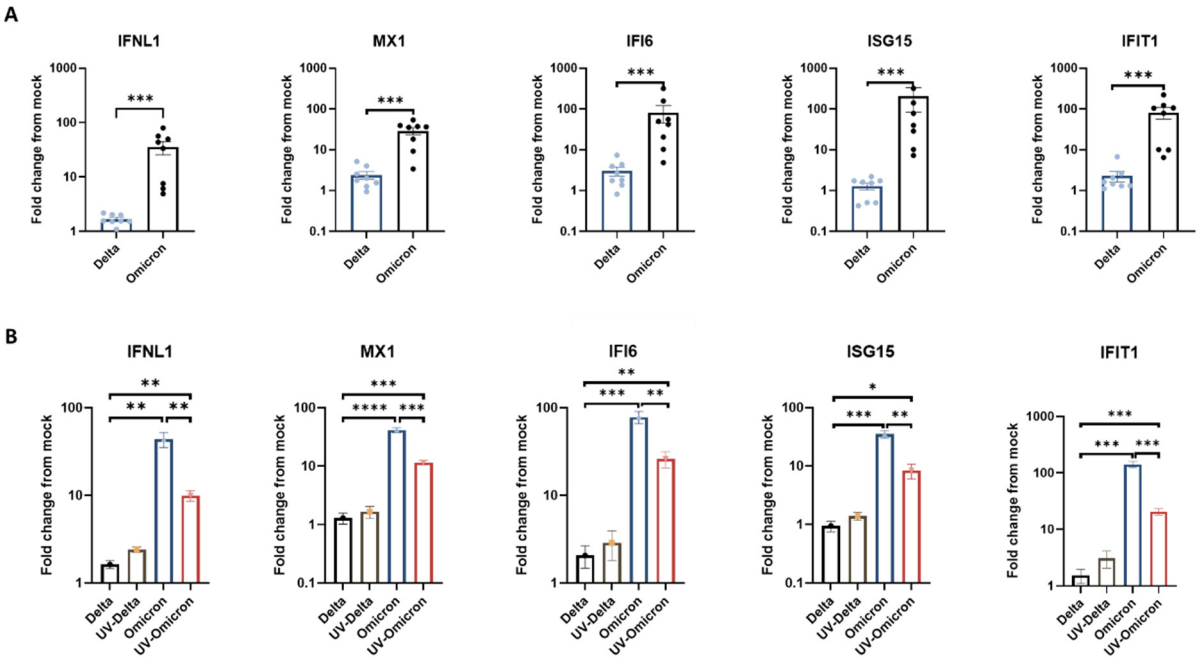

Figure 2. Lung tissue interferon response to SARS-CoV-2 Omicron and Delta. Lung organ cultures were infected in parallel with Omicron and Delta (10^5 PFU/well), and the effect of infection on the expression of the indicated innate immunity genes, measured by RT-qPCR at 24h post-infection, is presented as fold-change from mock-infection. (**A**) the mean values (±SEM) in 8 independent tissues, each tested in 4 biological replicates. (**B**) the mean values (±SEM) in a representative tissue (tested in 4 biological replicates) exposed in parallel to infectious versus UV-inactivated viruses. The results shown in panel B represent at least three independent tissues. *, $p < 0.05$; **, $p < 0.01$; ***, $p < 0.001$; ****, $p < 0.0001$.

In order to further define whether the relative enhancement of the innate response to Omicron in the lung tissues was dependent on active viral replication, we compared the induction of ISG following exposure to infectious versus UV-inactivated Omicron and Delta virions. Surprisingly, a significant induction of ISG was observed following exposure of the lung tissues to UV-inactivated Omicron (but not Delta) virions (Figure 2B),

despite the absence of de-novo viral gene expression (Figure S4). This finding indicated that the enhanced lung-tissue response to Omicron is already triggered, at least in part, by virion structural component/s upon initial virus-cell contact or entry, preceding viral gene expression.

3.3. Blocking the Innate Immune Signaling Restores Omicron Replication in the Lung Tissues

Finally, to assess the impact of the enhanced interferon response to Omicron on the observed restriction of Omicron replication in the lung tissues, we pretreated the lung organ cultures with the Janus kinase (JAK) 1/2 inhibitor ruxolitinib for 16 h before infection. We found that ruxolitinib treatment significantly inhibited ISG induction following infection (Figure S5). Notably, we found that ruxolitinib treatment significantly enhanced the levels of Omicron replication in the lung tissues with a more than 100-fold increase in Omicron infectious virus titers (bringing Omicron-to-near-Delta replication levels) (Figure 3). The same treatment only minimally affected the already efficient lung-tissue replication of Delta (with a ~5-fold increase in infectious virus titers). These results suggest that the enhanced innate immune response to Omicron plays a role in the specific restriction of Omicron (compared to other VOC) replication in the lung tissue.

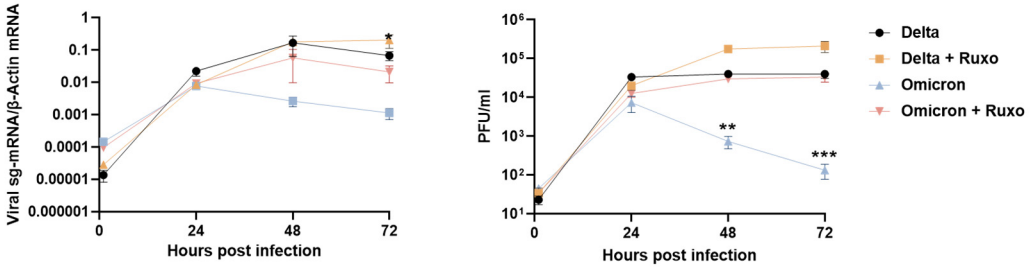

Figure 3. Ruxolitinib treatment restores Omicron replication in human lung tissues. Lung organ cultures were pretreated with 5 uM Ruxolitinib (Ruxo) 16 h when indicated. Treated and non-treated tissues were infected in parallel with Omicron and Delta (10^5 PFU/well). The levels of tissue-associated viral sub-genomic (sg)-mRNA (left panel) and infectious virus progeny released from the same infected tissue (right panel) represent mean values (±SEM) of four biological replicates. **, $p < 0.01$; ***, $p < 0.001$.

4. Discussion

Omicron infection was characterized by decreased clinical severity, raising the question of whether early variant-specific interactions within the mucosal surfaces of the respiratory tract could mediate its attenuated pathogenicity. Using our ex vivo infection models of native human lung and nasal tissues, we show that the replication competence of Omicron in lung tissues is highly restricted compared to Delta and precedent VOC, whereas it remains relatively unchanged in nasal tissues. The high susceptibility of the nasal viral entry site to Omicron may support person-to-person transmission, whereas the restricted replication in the lungs could contribute to the milder clinical course of Omicron.

Our findings reveal a new potential mechanism, whereby the significantly enhanced antiviral interferon responses to Omicron compared to earlier VOC, which was most striking in the lung tissues (where the innate immune response to all other SARS-CoV-2 VOC was blunted), could limit its replication and potential pathogenicity in the lower respiratory tract. The differences in the interferon response triggered by Omicron versus Delta in the nasal tissues were less remarkable, as the interferon response in the nasal tissues was already significantly induced by Delta and only mildly further induced by Omicron (Figure S3). Accordingly, this additional modest increment of ISG induction did not appear to be associated with significant differences in the replication capacity between Delta and Omicron in the nasal tissues (Figure 1A).

Innate immune defenses were shown to play a crucial role in the control of SARS-CoV-2 infection, and impaired local interferon responses in the respiratory tract have

been associated with severe COVID-19 [14,15,18]. Hence, an augmented mucosal innate immune response to Omicron could capture the virus at the upper respiratory tract and limit viral replication and consequent pathology in the lungs. In addition to the upregulated ISG, the observed induction of IFNλ by Omicron in the nasal and lung tissues (Figure 2 and Figure S3) is noteworthy, given the reported key role of mucosal IFNλ in the protection against infection and excessive inflammation caused by SARS-CoV-2 variants (including Omicron) in animal models, and in the protection against life-threatening COVID-19 in humans [16,20]. A similar effect in antiviral protection, as well as in the prevention of excessive inflammatory damage, was reported for IFNλ in experimental influenza infection [21]. Moreover, we directly showed that the enhanced lung tissue response to Omicron (versus Delta) was already triggered by UV-inactivated virus (incapable of viral gene expression) and that ruxolitinib pretreatment, reducing the ISG response to Omicron, significantly enhanced Omicron replication in the lung tissues, bringing Omicron replication to Delta replication levels (Figure 3). Collectively, our finding that the interferon response to Omicron was already triggered by virion structural components upon initial viral attachment/entry and that blocking the viral-induced innate immune signaling restored Omicron replication in the lung tissues imply a causative relation between the enhanced early antiviral response triggered by Omicron (compared to other VOC) and the restricted spread of Omicron in lung tissues. The relative early enhancement of the innate immune response may be related to the predominant use of the endocytic entry pathway by Omicron (as opposed to Delta) [2,10,12,13], which could lead to early activation of unique endosomal Toll-like receptors. The mechanism by which Omicron triggers the enhanced interferon response in human respiratory tissues remains to be elucidated.

Our study has several limitations. Native respiratory tissues in organ culture are relatively short-lived (up to 7 days in culture). Thus, our ex vivo infection models mirror early events of infection and do not address the late phase of viral transmission or the combined effects of the local and systemic immune responses. Nonetheless, our studies recapitulate SARS-CoV-2 infection and innate immune response within the authentic multicellular complexity of both the upper and the lower human respiratory tract, containing tissue-specific compositions of cell types, including immune cells and extracellular matrix. Currently, we are not aware of studies that have examined the distinctive innate tissue responses to Omicron as related to its altered replication phenotype in the lower respiratory tract. Such data are critical to better understand and address the evolution of SARS-CoV-2 into a less virulent human-tropic virus.

In summary, our studies in native human nasal and lung tissues infected ex vivo reveal a significantly enhanced interferon response to Omicron compared to precedent SARS-CoV-2 VOC. The findings imply that the early induction of antiviral ISG, which was most prominent in lung tissues (where it was specific to Omicron), could play a part in the restricted replication and pathology of Omicron in the lungs. They provide insights into the attenuated pathogenicity of Omicron and for further studies of pathways involved in the enhanced mucosal innate immune responses to this evolving variant.

Supplementary Materials: The following supporting information can be downloaded at: https://www.mdpi.com/article/10.3390/v14071583/s1, Figure S1: Replication kinetics of SARS-CoV-2 variants in human lung tissues; Figure S2: Lung tissue ISG response to SARS-CoV-2 variants and influenza; Figure S3: Nasal tissue ISG response to SARS-CoV-2 Omicron and Delta; Figure S4: Viral subgenomic (sg)-mRNA in lung tissues exposed to infectious versus UV-inactivated SARS-CoV-2 Omicron and Delta; Figure S5: Effect of Ruxolitinib on lung tissue ISG response to Omicron infection; Table S1: Primers and probes for real-time PCR analysis;

Author Contributions: Conceptualization, D.G.W., A.P. and O.A; methodology, O.A. and D.G.W.; software, S.A. and H.G.B.; investigation, O.A., M.H., O.W. (Ori Wandel), E.O.-D. and O.V.; resources, O.W. (Ori Wald), A.Y., B.G., H.K., N.R. and M.M.; data curation, O.A., M.H., Z.Z.-R. and M.O.; writing—original draft preparation, O.A., D.G.W. and A.P.; writing—review and editing, D.G.W.; supervision, D.G.W. and A.P.; project administration, D.G.W.; funding acquisition, D.G.W., A.P. and O.W. (Ori Wald). All authors have read and agreed to the published version of the manuscript.

Funding: This research was funded by the Israel Science Foundation, grant numbers 530/18 and 1728/20, the Israel Ministry of Science and Technology (3-16964), and the Hadassah France Association.

Institutional Review Board Statement: The study was approved by the Institutional Review Board of Hadassah Medical Center (#0296-20-HMO) and the Sheba Medical Center (#2832-15-SMC).

Informed Consent Statement: Informed consent was obtained from all subjects involved in the study.

Data Availability Statement: All the sequences of the virus isolates used are available in GISAID. The accession numbers of viral sequences used in this study are listed above. The raw data for all graphs presented in this paper are included as source data.

Conflicts of Interest: The authors declare no conflict of interest.

References

1. Cele, S.; Jackson, L.; Khoury, D.S.; Khan, K.; Moyo-Gwete, T.; Tegally, H.; San, J.E.; Cromer, D.; Scheepers, C.; Amoako, D.G.; et al. Omicron extensively but incompletely escapes Pfizer BNT162b2 neutralization. *Nature* **2022**, *602*, 654–656. [CrossRef] [PubMed]
2. Sigal, A. Milder disease with Omicron: Is it the virus or the pre-existing immunity? *Nat. Rev. Immunol.* **2022**, *22*, 69–71. [CrossRef] [PubMed]
3. Muik, A.; Lui, B.G.; Wallisch, A.-K.; Bacher, M.; Mühl, J.; Reinholz, J.; Ozhelvaci, O.; Beckmann, N.; Garcia, R.d.l.C.G.; Poran, A.; et al. Neutralization of SARS-CoV-2 Omicron by BNT162b2 mRNA vaccine–elicited human sera. *Science* **2022**, *7591*, eabn7591. [CrossRef] [PubMed]
4. da Silva, S.J.R.; Kohl, A.; Pena, L.; Pardee, K. Recent insights into SARS-CoV-2 omicron variant. *Rev. Med. Virol.* **2022**, e2373. [CrossRef] [PubMed]
5. Wolter, N.; Jassat, W.; Walaza, S.; Welch, R.; Moultrie, H.; Groome, M.; Amoako, D.G.; Everatt, J.; Bhiman, J.N.; Scheepers, C.; et al. Early assessment of the clinical severity of the SARS-CoV-2 omicron variant in South Africa: A data linkage study. *Lancet* **2022**, *399*, 437–446. [CrossRef]
6. Public Health England. *SARS-CoV-2 Variants of Concern and Variants under Investigation in England*; Sage: Newcastle upon Tyne, UK, 2021; Volume 1, pp. 1–50.
7. McMahan, K.; Giffin, V.; Tostanoski, L.H.; Chung, B.; Siamatu, M.; Suthar, M.S.; Halfmann, P.; Kawaoka, Y.; Piedra-Mora, C.; Jain, N.; et al. Reduced pathogenicity of the SARS-CoV-2 omicron variant in hamsters. *Med* **2022**, *3*, 262–268.e4. [CrossRef] [PubMed]
8. Bentley, E.G.; Kirby, A.; Sharma, P.; Kipar, A.; Mega, D.F.; Bramwell, C.; Penrice-Randal, R.; Prince, T.; Brown, J.C.; Zhou, J.; et al. SARS-CoV-2 Omicron-B.1.1.529 Variant Leads to Less Severe Disease than Pango B and Delta Variants Strains in a Mouse Model of Severe COVID-19. *bioRxiv* **2021**. [CrossRef]
9. Abdelnabi, R.; Foo, C.S.; Zhang, X.; Lemmens, V.; Maes, P.; Slechten, B.; Raymenants, J.; André, E.; Weynand, B.; Dallmeier, K.; et al. The omicron (B.1.1.529) SARS-CoV-2 variant of concern does not readily infect Syrian hamsters. *Antivir. Res.* **2022**, *198*, 105253. [CrossRef] [PubMed]
10. Lamers, M.M.; Mykytyn, A.Z.; Breugem, T.I.; Groen, N.; Knoops, K.; Schipper, D.; van Acker, R.; van den Doel, P.B.; Bestebroer, T.; Koopman, C.D.; et al. SARS-CoV-2 Omicron efficiently infects human airway, but not alveolar epithelium. *bioRxiv* **2022**. [CrossRef]
11. Hui, K.P.Y.; Ho, J.C.W.; Cheung, M.-C.; Ng, K.-C.; Ching, R.H.H.; Lai, K.-L.; Kam, T.T.; Gu, H.; Sit, K.-Y.; Hsin, M.K.Y.; et al. SARS-CoV-2 Omicron variant replication in human bronchus and lung ex vivo. *Nature* **2022**, *603*, 715–720. [CrossRef] [PubMed]
12. Willett, B.J.; Grove, J.; Maclean, O.A.; Wilkie, C.; Logan, N.; De, G.; Furnon, W.; Scott, S.; Manali, M.; Szemiel, A.; et al. The hy-per-transmissible SARS-CoV-2 Omicron variant exhibits significant antigenic change, vaccine escape and a switch in cell entry mechanism. *medRxiv* **2022**, 1–59. [CrossRef]
13. Peacock, T.P.; Brown, J.C.; Zhou, J.; Thakur, N.; Newman, J.; Kugathasan, R.; Sukhova, K.; Kaforou, M.; Bailey, D.; Barclay, W.S. The SARS-CoV-2 Variant, Omicron, Shows Rapid Replication in Human Primary Nasal Epithelial Cultures and Efficiently Uses the Endosomal Route of Entry. *bioRxiv* **2022**. [CrossRef]
14. Bastard, P.; Zhang, Q.; Zhang, S.-Y.; Jouanguy, E.; Casanova, J.-L. Type I interferons and SARS-CoV-2: From cells to organisms. *Curr. Opin. Immunol.* **2022**, *74*, 172–182. [CrossRef] [PubMed]
15. Ziegler, C.G.K.; Miao, V.N.; Owings, A.H.; Navia, A.W.; Tang, Y.; Bromley, J.D.; Lotfy, P.; Sloan, M.; Laird, H.; Williams, H.B.; et al. Impaired local intrinsic immunity to SARS-CoV-2 infection in severe COVID-19. *Cell* **2021**, *184*, 4713–4733.e22. [CrossRef] [PubMed]
16. Sposito, B.; Broggi, A.; Pandolfi, L.; Crotta, S.; Clementi, N.; Ferrarese, R.; Sisti, S.; Criscuolo, E.; Spreafico, R.; Long, J.M.; et al. The interferon landscape along the respiratory tract impacts the severity of COVID-19. *Cell* **2021**, *184*, 4953–4968.e16. [CrossRef] [PubMed]
17. Alfi, O.; Yakirevitch, A.; Wald, O.; Wandel, O.; Izhar, U.; Oiknine-Djian, E.; Nevo, Y.; Elgavish, S.; Dagan, E.; Madgar, O.; et al. Human Nasal and Lung Tissues Infected Ex Vivo with SARS-CoV-2 Provide Insights into Differential Tissue-Specific and Virus-Specific Innate Immune Responses in the Upper and Lower Respiratory Tract. *J. Virol.* **2021**, *95*, e0013021. [CrossRef] [PubMed]

18. Martin-Sancho, L.; Lewinski, M.K.; Pache, L.; Stoneham, C.A.; Yin, X.; Pratt, D.; Churas, C.P.; Rosenthal, S.B.; Liu, S.; De Jesus, P.; et al. Functional Landscape of SARS-CoV-2 Cellular Restriction. *Mol. Cell* **2020**, *81*, 2656–2668.e8. [CrossRef]
19. Beyer, D.K.; Forero, A. Mechanisms of Antiviral Immune Evasion of SARS-CoV-2. *J. Mol. Biol.* **2022**, *434*, 167265. [CrossRef] [PubMed]
20. Chong, Z.; Karl, C.E.; Halfmann, P.J.; Kawaoka, Y.; Winkler, E.S.; Keeler, S.P.; Holtzman, M.J.; Yu, J.; Diamond, M.S. Nasally delivered interferon-λ protects mice against infection by SARS-CoV-2 variants including Omicron. *Cell Rep.* **2022**, *39*, 110799. [CrossRef] [PubMed]
21. Galani, I.E.; Triantafyllia, V.; Eleminiadou, E.-E.; Koltsida, O.; Stavropoulos, A.; Manioudaki, M.; Thanos, D.; Doyle, S.E.; Kotenko, S.V.; Thanopoulou, K.; et al. Interferon-λ Mediates Non-redundant Front-Line Antiviral Protection against Influenza Virus Infection without Compromising Host Fitness. *Immunity* **2017**, *46*, 875–890.e6. [CrossRef] [PubMed]